Journal of *Marine Science and Engineering*

MDPI

Article

Diffusion and Superposition of Ship Exhaust Gas in Port Area Based on Gaussian Puff Model: A Case Study on Shenzhen Port

Langxiong Gan [1,2,3], Tianfu Lu [1,2] and Yaqing Shu [2,3,*]

[1] Hainan Institute, Wuhan University of Technology, Sanya 572000, China
[2] School of Navigation, Wuhan University of Technology, Wuhan 430063, China
[3] Hubei Key Laboratory of Inland Shipping Technology, Wuhan 430063, China
* Correspondence: y.shu@whut.edu.cn

Abstract: Ship exhaust gas has become an essential source of air pollution in recent years. To assess the impact of ship exhaust gas on the atmospheric environment and human health, this paper studies the problem of ship exhaust gas diffusion in the port area. According to automatic identification system (AIS) data, ship exhaust gas is estimated based on the bottom-up method, and the result of emission calculation is entered into a Gaussian puff model to calculate the superposition of the diffusion of gaseous pollutants from multiple ships. In addition, the results of a case study of the diffusion of ship exhaust gas in the western area of Shenzhen Port in China show that the distribution of the NO_2 concentration in the studied area is not stable, the diffusion of exhaust gas from multiple ships mainly affects some areas near large ship berths at night, and there is a small impact on the whole study area. This lays a foundation for monitoring and treating the atmospheric environment in the port area.

Keywords: ship exhaust gas; Gaussian puff model; diffusion simulation; air pollution

Citation: Gan, L.; Lu, T.; Shu, Y. Diffusion and Superposition of Ship Exhaust Gas in Port Area Based on Gaussian Puff Model: A Case Study on Shenzhen Port. *J. Mar. Sci. Eng.* **2023**, *11*, 330. https://doi.org/10.3390/jmse11020330

Academic Editors: Gerardo Gold Bouchot and Alberto Ribotti

Received: 21 December 2022
Revised: 23 January 2023
Accepted: 26 January 2023
Published: 3 February 2023

1. Introduction

Ships consume significant amounts of energy during operation, resulting in an exhaust emission problem that needs to be addressed. Statistics indicate that the annual carbon dioxide (CO_2) emissions caused by maritime transport are estimated at 1 billion tons [1], and NO_X and SO_X emissions may account for 15% and 5–8%, respectively, of global total emissions [2]. Therefore, the problem of ship emissions has become a significant concern for researchers worldwide. To reduce emissions and improve air quality, the International Maritime Organization (IMO) has proposed the Ship Emission Control Area (ECA) policy, establishing four ECAs: the Baltic Sea, the North Sea, the English Channel, and the North American and the United States Caribbean coasts. The ECA regulation requires ships to use fuels with a sulfur content of no more than 0.1% within the ECA [3,4]. To further reduce emissions, IMO also limits the sulfur content of marine fuels outside the ECA to less than 0.5% [5]. In 2018, the Chinese government designated the entire area within 12 nautical miles of the Chinese coast as an emission control area; the sulfur content of ship fuel was initially limited to 0.5%, but was changed to 0.1% after 2020 [6].

The ECA policy has significantly reduced sulfur emissions from ships; however, the composition of pollutants in ship emissions is complex, and ship emissions significantly impact the ecological environment and people's health. Large amounts of CO_2 and CH_4 emitted by ships lead to global warming, and the deposition of sulfur oxides and nitrogen oxides lead to acid rain, soil acidification, and nitrogen enrichment. For example, ship emissions have led to a 15% increase in sulfate and nitrate deposition in Europe [7]. In addition, nitrogen dioxide (NO_2), SO_2, and $PM_{2.5}$ emitted from ships can also cause diseases such as asthma, bronchitis, and cardiovascular diseases. Research [8] shows that emissions from ocean vessels in East Asia were associated with approximately

14,500–37,500 premature deaths in 2013. Therefore, there is significant value in researching the pollution diffusion of ship exhaust emission.

The issue of ship emissions has attracted researchers for many years. Previous research on ship emissions has mainly focused on assessing the inventory of ship emissions and their impact on the environment and human health. There are currently two kinds of methods for establishing a ship emissions inventory: the top–down method and the bottom–up method.

The "top–down" method multiplies the total fuel consumption of the ship and emission factors of fuel to calculate the emissions [9]. For example, Corbett et al. [10] and Endresen et al. [11] used the top–down method to calculate the emissions in a large area. Jalkanen et al. [12] and Ng et al. [13] noted that this method is useful for obtaining preliminary estimates of local emissions, but the results must be verified by using bottom–up methods. When accurate ship traffic flow information is not available, emissions can be calculated by using a top–down method based on fuel statistics. The "bottom–up" method calculates the ship emissions based on ship activity, which considers the ship engine's power, fuel consumption rate, and emissions factor. The bottom–up method requires a large amount of ship data. After the introduction of the AIS, more AIS data have improved the accuracy of bottom–up method calculations [14]. Xing et al. [15] calculated ship emissions on the same route and concluded that the "top–down" method is more operational, but the "bottom–up" method is more accurate.

Researchers most commonly apply the "bottom–up" method to investigate the exhaust emissions across an entire water area, including multiple ports. Jalkanen et al. [16] calculated the ship emissions of the Baltic Sea based on the ship traffic emission assessment model (STEAM). Ng et al. [13] established the first new emission inventory of ocean-going vessels for Hong Kong based on AIS data. Fan et al. [17] applied this approach to estimate ship emissions in the Yangtze River Delta and East China Sea. Wan et al. [18] used a bottom–up methodology to study the emissions of the Yangtze River Delta, the Pearl River Delta, and Bohai Bay based on the data of ships berthing in Chinese ports in 2018. However, most studies have mainly focused on emissions and the emission contribution rate, and the pollution transfer effect of ship exhaust emission diffusion on land has not been explored. The air quality model is a mathematical and physical method to simulate the diffusion and reaction of air pollutants in time and space, which can provide enough of a scientific basis for monitoring emissions and assessing future environmental governance.

Examples of common air quality models include the Gaussian model, atmospheric dispersion modeling system (ADMS), AMS/EPA regulatory model (AERMOD), community multiscale air quality (CMAQ), etc. Different atmospheric diffusion models are developed for different purposes, with differences in principles, theories, and application scope [19]. ADMS and AERMOD are developed from the Gaussian model, and they are highly advanced and complex [20]; the main differences between them and the Gaussian model is ADMS and AERMOD simulate the chemical transformation process in the diffusion process. CMAQ simulates various chemical and physical processes, which have been designed to approach air quality as a whole [21]. Gaussian models are much simpler to use in practice, requiring less computer time to operate. Some studies used the Gaussian model to analyze the atmospheric diffusion of ship exhaust gas. Ariana et al. [22] pioneered the use of the Gaussian plume and Gaussian puff models to simulate and estimate the concentration distribution of ship emission diffusion based on ship AIS data. Bai et al. [23] combined the Gaussian model with ship AIS data to simulate the diffusion of air pollution within 2 km of a single ship. Murena et al. [24] used the Gaussian CALPUFF model to assess the impact of a cruise ship on air quality based on ship activity data. Peng et al. [25] studied the simulation calculation method of ship emission diffusion based on the Gaussian model and conducted empirical tests through a single ship application and shore-based monitoring stations. At present, there are many research studies on pollutants discharged by a single ship, but there is a lack of research on diffusion and superposition of exhaust gas from multiple ships in the port area.

In general, the large flow of ships in port waters will generate a large amount of exhaust gas. Moreover, the density of port cities is relatively high; that is, the emissions from ships in port areas harm more people's health. Considering the above characteristics, this paper studies the diffusion of ship exhaust gas in the port area, which helps analyze the harm caused by the diffusion of ship exhaust gas. This lays a foundation for monitoring and treating the atmospheric environment in the port area.

In this paper, the diffusion of ship exhaust gas in the port area is constructed and applied in this paper. First, the diffusion model of ship exhaust gas in port area is designed with a Gaussian puff model. Then, ship exhaust gas is estimated based on the bottom–up method and AIS data. Finally, the computed result of gas calculation is entered into Gaussian puff model to calculate the superposition of the diffusion of gaseous pollutants from multiple ships.

The remainder of this paper is organized as follows. The literature review on the calculation of ship emissions and air quality models is conducted in Section 1. In Section 2, the construction method of ship exhaust gas diffusion in the port area is introduced. In Section 3, a case study of the diffusion of multi-ship exhaust gas in the western area of Shenzhen Port, China is conducted, followed by a comprehensive discussion in Section 4. In Section 5, the conclusion is drawn.

2. Methodology

About 75% of ship emissions are discharged within the sea area 400 km away from the coastline [26]. When ships berth at the port, the ship emissions will make the SO_2 concentration in coastal areas increase by 10~50% [27]; this significantly impacts the ecological environment and resident health in coastal areas. To effectively control the pollution problem caused by ship emissions, it is important to determine the distribution of ship air pollutant concentrations. Given the problems above, this paper studies the diffusion of pollutants discharged by ships in the port area. This is done by using an air quality model to calculate the superposition of the diffusion of gaseous pollutants from multiple ships and obtain the small-scale distribution patterns of ship pollutant concentrations in the port area. This lays the groundwork for monitoring and treating air pollutants from ships in the port area.

In contrast to industrial emission sources on land, the diffusion patterns of ship emissions are highly related to their navigation status. When a ship is navigating, it is a moving emission source; when it is at anchor or at berth, the emission position is relatively fixed. Compared with road emission sources, ships can choose any route when navigating in open waters; therefore, the location of ship emission sources is random. AIS data include the position information and status information of the ship, so combining AIS data to calculate ship emissions can match the characteristics of ship emissions sources.

The diffusion of ship exhaust pollutants can be simulated by entering the ship emission source as a parameter into a gas diffusion model. Simulating the diffusion superposition effect of exhaust pollutants from multiple ships in the port area can generate distribution patterns of pollutant concentrations from ships in that small scale area. The technical method in this study is shown in Figure 1. This paper studies the problem of ship exhaust gas diffusion in the port area but does not analyze changes in gaseous pollutants. This is done mainly by simulating the diffusion and superposition of exhaust pollutants from multiple ships and analyzing the impact of pollution diffusion from ships on the port area.

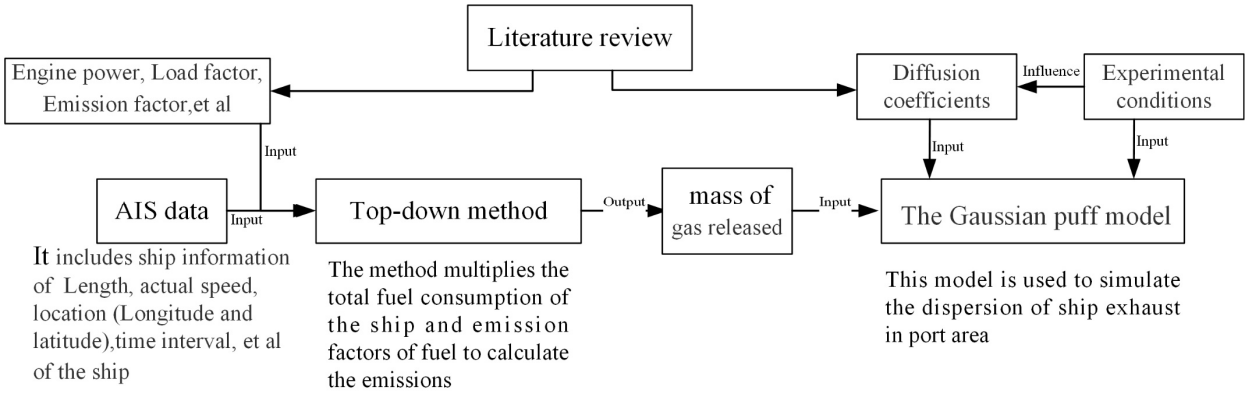

Figure 1. Technical method of diffusion model and calculation model of exhaust gas.

2.1. Mathematical Model

2.1.1. Diffusion Model

AIS data include the reported time and geographic coordinates. From these data, the ship emission trajectory can be considered to be a moving discrete point source. According to the time interval between two consecutive AIS reports for a ship's AIS data, combined with the bottom–up method to calculate the ship's emissions in this time period, the discharge location is considered to be the last point of two consecutive AIS reports. Based on the geographical coordinates, the ship emissions between two consecutive AIS reporting points can be considered to be pollutants discharged at a fixed location. Therefore, the pollutant discharges from all ships in the port area can be summarized based on the time and space data.

The sea and the coast are flat and open, and the diffusion mode of pollutants discharged by ships is relatively simple. Therefore, in this paper, the widely used Gaussian diffusion model is used to simulate the dispersion of ship exhaust. For the puff discharged by the ship at time t_s, the three-dimensions coordinate system was established. The original point is the vertical projection of the center of puff. The downwind direction was taken as the x-axis, crosswind as the y-axis, and vertical as the z-axis. With the assumption of 100% ground reflection and no deposition, the concentration of $C(x, y, z)$ can be seen as the superposition of the diffusion from the puff $(0, 0, H)$ and $(0, 0, -H)$ under the assumption of 100% ground reflection and no deposition, as shown in Figure 2:

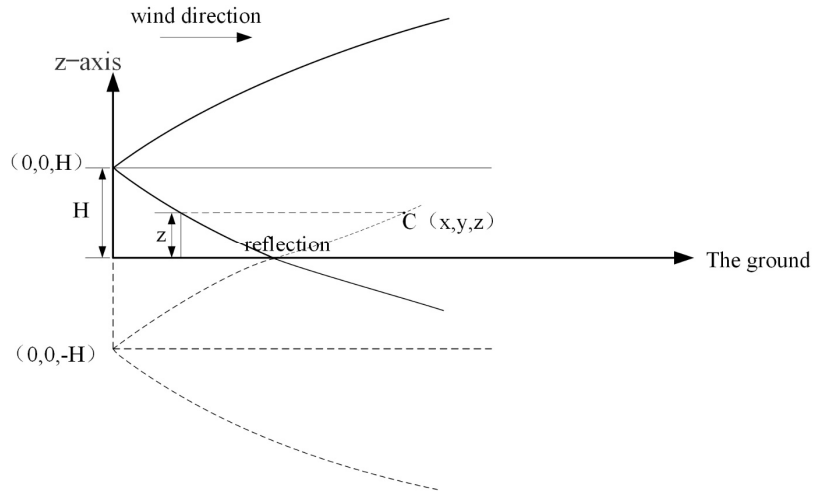

Figure 2. The sketch map of reflection.

The concentration of a spot (x, y, z) at the spatial at time t is calculated using the Gaussian puff model [28], as shown in Equation (1):

$$C(x,y,z,t) = \frac{Q}{(2\pi)^{3/2}\sigma_x\sigma_y\sigma_z} \exp\left[-\frac{(x-\overline{u}(t-t_s))^2}{2\sigma_x^2}\right] \cdot \exp\left(-\frac{y^2}{2\sigma_y^2}\right) \cdot \left\{\exp\left[-\frac{(z-H)^2}{2\sigma_z^2}\right] + \exp\left[-\frac{(z+H)^2}{2\sigma_z^2}\right]\right\} \quad (1)$$

where $\sigma_x, \sigma_y, \sigma_z$ is the diffusion coefficient of the leakage gas in downwind, crosswind, and vertical directions, respectively, which is related to the downwind distance x, measured in the unit m; H is the effective height of the puff, also in the unit m; $C(x, y, z)$ is the concentration of leakage gas at any point, measured in the unit of kg/m^3; $\overline{u}$ is the wind speed at a unit of m/s; Q is the total mass of gas released (source strength) in a unit of kg; t_s is the time of the puff discharged by the ship; and t is the time after t_s. The unit of t_s and t is the Unix timestamp.

Assume the ship sails until time t_m. The concentration at the spatial point (x', y', z') at time t_m is the superimposition of the concentration from n puffs discharged by the ship at time $t, t_1, t_2, \cdots\cdots t_m$.

2.1.2. Calculation Model of Exhaust Gas

According to AIS data, this paper uses the bottom–up method to calculate ship exhaust gas. The method multiplies the output power of the ship's equipment with the corresponding emission factor and load factor, and then multiplies that by the working time to calculate the ship's exhaust emissions under different sailing conditions. The estimation formula is as follows:

$$E_{i,j,k,l} = \sum_{i=1}^{n} P_j \times LF_{j,l} \times T_{j,l} \times EF_{i,j,k} \times LLAF_j / 10^6 \quad (2)$$

where i represents the type of pollutants in the tail gas (such as SO_2 and NO_X); j represents the engine type (main engine (ME) or auxiliary engine (AE)); k represents fuel type (heavy fuel oil (HFO), marine diesel oil (MDO), marine gas oil (MGO) or general diesel oil (GDO)); l represents the operating mode (normal cruising, slow-steaming, maneuvering, anchoring or berthing); n represents the number of AIS reports; E is the calculated emissions, with a unit of t; P is the rated power, with a unit of kW; LF is the load factor; T is the working time, with a unit of h; EF is the emission factor, with a unit of g/kW·h; and $LLAF$ is the adjustment factor of a low load (main engine only).

In addition, the behavioral characteristics and ship parameters of fishing ships are unique, with the following model for calculating emissions:

$$E_{i,j,l} = EF_i' \times \sum (P_l \times F_{j,l} \times T) \quad (3)$$

In this formula, the definitions of i, j, l, E, P are in common with the parameters in Equation (2). EF' is the emission factor of fishing ships, with a unit of kg/t; F is the average consumption of fuel, with a unit of g/kW·h; and T' is the working hours of fishing ships.

2.2. Model Parameters

2.2.1. Parameters of Diffusion Model

The total mass Q of the gas released within a specific time is related to the ship emissions and is calculated using a top–down method based on AIS data. Wind speed and direction are calculated using meteorological forecasts or observations. The diffusion parameter adopts the empirical formula of Bridges in the open plain field [29]. The parameters are listed in Table 1. In Table 1, d is the distance of downwind direction, σ_x, σ_y are the horizontal diffusion coefficients, respectively, and σ_z is the vertical diffusion coefficient.

Table 1. Table of diffusion coefficients.

Atmospheric Stability	σ_x/σ_y	σ_z
A	$0.22d/(1+0.0001d)^{0.5}$	0.2d
B	$0.16d/(1+0.0001d)^{0.5}$	0.12d
C	$0.11d/(1+0.0001d)^{0.5}$	$0.08d/(1+0.0001d)^{0.5}$
D	$0.08d/(1+0.0001d)^{0.5}$	$0.06d/(1+0.0001d)^{0.5}$
E	$0.06d/(1+0.0001d)^{0.5}$	$0.03d/(1+0.0001d)^{0.5}$
F	$0.04d/(1+0.0001d)^{0.5}$	$0.016d/(1+0.0001d)^{0.5}$

The gas diffusion coefficient is directly related to atmospheric stability. This study uses the classification grades of atmospheric stability in the Technical Methods for Formulating Local Emission Standards of Air Pollutants GB/T 3840-91 [30]. The grades, listed in Table 2, include six levels: strong instability, instability, weak instability, neutral, relatively stable, and stable, represented as A, B, C, D, E, and F, respectively.

Table 2. Grade of atmospheric stability.

Ground Wind Speed m/s	Intensity of Solar Radiation					
	+3	+2	+1	0	−1	−2
≤1.9	A	A–B	B	D	E	F
2–2.9	A–B	B	C	D	E	F
3–4.9	B	B–C	C	D	D	E
5–5.9	C	C–D	D	D	D	D
≥6	D	D	D	D	D	D

The ground wind speed (m/s) refers to the 10 min average wind speed at a height of 10 m above the ground. The intensity of solar radiation is related to cloud fraction and solar altitude; these can be determined by Table 3 according to GB/T 3840-91.

Table 3. Determination of intensity of solar radiation.

Total Cloud Cover/Low Cloud Cover	At Night	Solar Altitude h			
		$h \leq 15^\circ$	$15^\circ < h \leq 35^\circ$	$35^\circ < h \leq 65^\circ$	$h > 65^\circ$
<4/≤4	−2	−1	+1	+2	+3
5–7/≤4	−1	0	+1	+2	+3
≥8/≤4	−1	0	0	+1	+1
≥7/≤5–7	0	0	0	0	+1
≥8/≥8	0	0	0	0	0

Total cloud cover and low cloud cover can be obtained from meteorological observation. Solar altitude is the angular height of the sun in the sky measured from the horizon [31].

2.2.2. Parameters of Emission Calculation

The "bottom–up" method calculates the ship emissions based on ship activity, which considers the engine power, fuel consumption rate, and emissions factor. Calculating ship emissions requires detailed activity data and attribute information of the ships. In the AIS data, the static data of ship include the name, call sign, MMSI (maritime mobile service identity), type, length, and other variables. The dynamic data of the ship include longitude and latitude, course, speed, draft, time stamp, and other variables. In this study, we used AIS data for Shenzhen Port from January to June 2018, purchased from www.shipxy.com (accessed on 10 December 2022).

(1) Engine power

The engine power of a ship is important datum for calculating ship emissions. However, accurate ship power data are often not disclosed, making it difficult to obtain them. When calculating ship emissions, this study refers to ship information published by the China Classification Society (CCS) and relevant research, divides the ships in port waters into inland ships, coastal ships, and ocean ships, and determines the calculation method of engine power as described in the following sections.

1) Main engine power

This paper selects a fitting formula based on the gross tonnage and main engine power to estimate the ship power of the main engine. The gross tonnage (GT) is estimated by the ship's length. The method [32] is presented in Tables 4 and 5.

Table 4. Relationship between length and GT.

	Ship Type	Relationship
Ocean ship	Cargo ship	$GT = 1.263L^2 - 117.31L + 6364$
	Tanker	$GT = 3.3301L^2 - 832.12L + 65284$
	Tug	$GT = 1.7228L^2 - 110.77L + 2223$
	Other	$GT = 0.9833L^2 - 98.586L + 5665$
Coastal ship	Cargo ship	$GT = 0.8444L^2 - 16.34L - 2368.1$
	Tanker	$GT = 1.9858L^2 - 309.62L + 13694$
	Tug	$GT = 1.568L^2 - 25.505L - 650.52$
	Other	$GT = 0.7053L^2 - 29.708L + 934.75$
Inland ship	Cargo ship	$GT = 0.3359L^2 + 3.8597L - 374.55$
	Tanker	$GT = 0.6542L^2 - 41.449L + 823.92$
	Tug	$GT = 0.5274L^2 - 7.2294L - 13.135$
	Other	$GT = 1.4979L^2 - 86.636L + 1459.1$
	Passenger ship	$GT = 0.0593L^{2.4315}$

Table 5. Relationship between GT and power.

	Ship Type	Relation
Ocean ship	Cargo ship	$P = 0.5903GT - 567.97$
	Tanker	$P = 0.1459GT + 4569$
	Tug	$P = 2.9991GT + 948.8$
	Other	$P = 0.5739GT + 2162.1$
Coastal ship	Cargo ship	$P = 0.3528GT + 71.174$
	Tanker	$P = 0.2063GT + 829.46$
	Tug	$P = 2.2203GT + 1568.8$
	Other	$P = 0.2966GT + 1301$
Inland ship	Cargo ship	$P = 0.3796GT + 30.154$
	Tanker	$P = 0.608GT + 16.081$
	Tug	$P = 8.7862GT - 565.64$
	Other	$P = 0.4625GT + 115.8$
	Passenger ship	200 kw (GT $\leq$ 200 t) 250 kw (GT $\leq$ 400 t) 510 kw (GT > 400 t)

Note: The recommended power of ocean passenger ships is 15,000 kW; for coastal passenger ships, it is 5000 kW.

To estimate the power of container ships, this study assumes that hull structures of container ships are highly similar (container ships are loaded with standard containers). Therefore, this study determines the power of container ships using fitting data published by the CCS. A total of more than 600 container

ships were selected for this study; we fit the relationship between the length and the GT of the ship, calculating the quantity relationship as follows:

$$GT = 0.001061L^{3.176} \quad (4)$$

where x is the length of ship and y is GT. Figure 3 shows the fitting results.

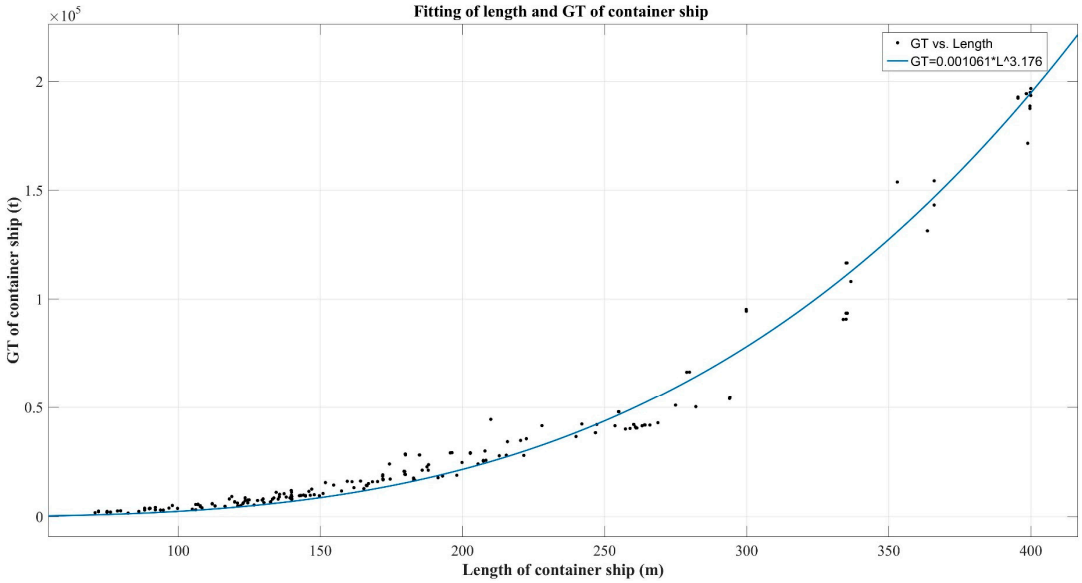

Figure 3. The relationship between the length and GT of container ship.

Based on the relationship between the length and GT, the fitted formula in the study [33] is selected to measure the relationship between GT and main engine power of the container ship:

$$P = 3.1907GT^{0.8493} \quad (5)$$

The engine power of the fishing ship is calculated using the Statistical Yearbook of Guangdong Province. In 2020, there were 2115 fishing ships in Shenzhen, with a total power of 110,728 kW. It is difficult to complete a detailed division of the types and operation modes; as such, this study uses the average value of 110,728/2115 =52.4 kW as the main engine power of an average fishing ship in Shenzhen Port.

2) Auxiliary engine power

Due to the shortage of information about the rated power of the auxiliary engine, the AE-rated power of a specific ship type is estimated by using the power ratio of AE to ME according to past experience with emission inventories. Based on [33], the power ratios used in this study are presented in Table 6.

Table 6. Power ratios of AE/ME.

Ship Type	Auxiliary Engine/Main Engine
Tanker	0.211
Cargo ship	0.220
Container ship	0.220
Tug	0.221
Passenger ship	0.278
Fishing ship	0.222
Other	0.222

(2) Running state of the ship's main engine

The running state of the ship's main engine is closely related to the sailing state and is an important factor for determining the engine emissions. The condition limits established to divide the ship's operational conditions are also presented in Table 7.

Table 7. Division of ship operation conditions.

Scheme	Normal Cruising	Slow-Steaming	Accessing Berth/Anchorage	Anchoring or Berthing
Speed limit	$v > 11$ kn	11 kn $\geq v \geq 6$ kn	1 kn $< v \leq 6$ kn	$v \leq 1$ kn

(3) Load factor

The load factor reflects the percentage of the mechanical power as a part of the rated power at different ship sailing speeds. The load factor of the main engine is related to the third power of speed. The estimation formula as follows:

$$LF = (AS/MS)^3 \quad (6)$$

where LF is the load rate (%), AS is the actual speed, and MS is the maximum speed of the ship.

The actual speed is obtained from AIS data; however, the maximum speed of the ship cannot be determined using this approach. Therefore, based on ship data published by the CCS and research results for the Pearl River Delta region [32], the maximum speeds of different ship types are shown in Table 8.

Table 8. Maximum speed of ships.

	Ship Type	Maximum Speed (kn)
Ocean ship	Container ship	21
	Tanker	16 [1)]
	Cargo ship	16
	Passenger ship	22
	Other	14.2
Coastal ship	Container ship	15
	Tanker	13
	Cargo ship	14
	High-speed passenger ship	42
	Other	11.5
Inland ship	Container ship	11
	Tanker	11
	Cargo ship	12
	Passenger ship	8.2
	Other	9.3

Note: [1)] small sample size; the values in the table may have errors when compared with actual data; in the calculation, if the normal speed in AIS data of a ship exceeds the values many times, the maximum speed of the ship is determined using AIS data.

The load of the main engine is low when the ship sails at a low speed. In this case, the combustion efficiency is low, leading to an increase in the pollutant emissions of the ship per unit time. To correct the ship emissions under a low load, we need to multiply it by the adjustment factor. In this study, when the load factor of the ship's main engine is lower than 20%, the low load adjustment multipliers (LLAM) are used to correct the emission factor. The value [34] is in Table A1. The formula is as follows:

$$EF_0 = EF_{i,j,k} \cdot LLAM \quad (7)$$

(4) Emission factor

Emission factor refers to the average emission rate of a particular pollutant emitted by a specific emission source. Emission factors for each exhaust pollutant were directly related to the engine type, fuel type, and sulfur content. The emission factor of the ship refers to past research [34]. Table A2 shows the values of emission factors.

Due to the special characteristics of fishing ships, the parameters for calculating their emissions need to be listed separately. It is difficult to classify the types and operation modes of fishing ships in detail; as such, the average fuel consumption of fishing ships is 500 g/kW·h. Emission factors of fishing ships draw from research on Shenzhen Port [35]; the value is detailed in Table A3.

3. Case Study

3.1. Simulation Experiment Design

3.1.1. Assumptions

(1) The atmospheric stability, wind speed, wind direction, and other meteorological conditions are stable during the study period;
(2) The theoretical premise of the Gaussian diffusion model is valid;
(3) Assume that the sea level and land are at the same level;
(4) The ship track is segmented based on the reported interval in AIS, and the emission generated in each segment is considered to be a puff;
(5) AIS data are normal data and errors are not considered.

3.1.2. Representative Pollutant and Damage

The pollutant composition of ship exhaust gas is complex; pollutants include COx, NOx, SOx, $PM_{2.5}$, and others. Under the action of wind, these pollutants drift to the land over time, damaging the ecological environment. To measure the impact of ship exhaust on land after diffusion, the technical regulation on ambient air quality index (on trial) (HJ 633-2012) [36] defines the air quality index (AQI), which is used to measure the degree of air pollution and the impact on human health, as shown in Table 9.

Table 9. The related description of AQI.

Air Quality Index	Air Quality Level	Health Impact on Residents
0–50	Excellent	Essentially no air pollution
51–100	Good	Some pollutants may have a weak impact on the health of a few highly sensitive people
101–150	Slight pollution	Symptoms of susceptible people are slightly aggravated, healthy people experience discomfort
151–200	Moderate pollution	May further aggravate the symptoms of susceptible people, may affect the heart and respiratory system of healthy people
201–300	Heavy pollution	Symptoms of patients with heart disease and lung disease are significantly aggravated, exercise tolerance is reduced, symptoms are common among healthy people
>300	Serious pollution	Healthy people have strong symptoms, and some diseases appear earlier than normal

The AQI is calculated using Equation (8):

$$AQI = \max\{IQAI_1, IQAI_2, \cdots, IQAI_n\} \quad (8)$$

where $IQAI$ is the individual air quality index, and n corresponds to the type of pollutant. The IAQI is an air quality index that describes a single pollutant. According to HJ 633-

2012, the pollutant concentrations corresponding to the values of IQAQ are listed in the following Table 10.

Table 10. Concentration limit of pollutants corresponding to IQAI.

Individual Air Quality Index	Concentration Limit of Pollutant							
	SO_2 24 h Average/ ($\mu g/m^3$)	SO_2 1 h Average/ ($\mu g/m^3$)	NO_2 24 h Average/ ($\mu g/m^3$)	NO_2 1 h Average/ ($\mu g/m^3$)	PM_{10} 24 h Average/ ($\mu g/m^3$)	CO 24 h Average/ ($\mu g/m^3$)	CO 1 h Average/ ($\mu g/m^3$)	$PM_{2.5}$ 24 h Average/ ($\mu g/m^3$)
0	0	0	0	0	0	0	0	0
50	50	150	40	100	50	2	5	35
100	150	500	80	200	150	4	10	75
150	475	650	180	700	250	14	35	115
200	800	800	280	1200	350	24	60	150
300	1600	1)	565	2340	420	36	90	250

Note: 1) the hourly average concentration of SO_2 is higher than 800 $\mu g/m^3$; the IAQI of SO_2 is reported as the 24 h average concentration.

A higher AQI value is associated with a higher level of air pollution. The AQI value is determined by the maximum IAQI among different pollutants based on Equation (8). There are many kinds of pollutants in ship exhaust. As such, determining the pollutant in the ship exhaust that most easily reaches the maximum IAQI value and simulating it as a representative pollutant effectively reflects the overall air quality and reduces the calculation burden.

IAQI is positively correlated with the concentration limits of different pollutants after the diffusion of ship exhaust, as shown in Table 9. Combined with Equation (1), it indicates that the concentration limit after pollutant diffusion is positively correlated with the quality of pollutants discharged from ships. Gan et al. [37] calculated the SO_X, NO_X, CO, PM_{10}, $PM_{2.5}$, and VOCs of ship emissions in the western area of Shenzhen Port in 2018, with results of 2683.1 t, 7273.0 t, 615.5 t, 398.6 t, 366.8 t, and 295.9 t, respectively. It indicates that NO_2 is most likely to reach a higher IAQI value (NO and NO_2 account for more than 90% of NOx [38], and NO is easily oxidized to NO_2). It can be considered that NOx diffusion is equivalent to NO_2 diffusion, so NO_2 is selected as the representative pollutant for this simulation, using the NO_2 concentrations exceeding 50 $\mu g/m^3$ (good air quality) and 100 $\mu g/m^3$ (slight pollution) to measure the degree of air pollution and the impact on human health.

In this paper, the reflection from the sea is not 100%, NO_2 reacts with water to produce HNO_3 and NO, and HNO_3 is soluble in water. It can be considered that the diffusion from the puff $(0, 0, -H)$ needed to be corrected. The reaction equation is as follows:

$$3NO_2 + H_2O \rightarrow 2HNO_3 + NO,\ 2NO + O_2 \rightarrow 2NO_2$$

It can be seen that HNO_3 is soluble in water. Moreover, NO is insoluble in water, and it is subsequently oxidized to NO_2. That is, if once reaction is considered, approximately two-thirds of NO_2 is absorbed and one-third of NO_2 is reflected from the sea.

So, it can be concluded that the correction factor is one-third, and that is 0.34 by maintaining two digits after decimal point. The reason we take 0.34 instead of 0.33 is as follows: (1) If once reaction is finished completely, at least one-third of NO_2 will be reflected. Since 0.33 is less than one-third, that is unreasonable. (2) We take 0.34 to be the correction factor; it can be explained as some of the NO_2 not being absorbed.

If once reaction is considered, Equation (1) is revised as follows:

$$X(x,y,z,t,H) = \frac{Q}{(2\pi)^{3/2}\sigma_x\sigma_y\sigma_z}\exp\left[-\frac{(x-\overline{u}(t-t_s))^2}{2\sigma_x^2}\right]\cdot\exp\left(-\frac{y^2}{2\sigma_y^2}\right)\cdot \left\{\exp\left[-\frac{(z-H)^2}{2\sigma_z^2}\right] + 0.34\exp\left[-\frac{(z+H)^2}{2\sigma_z^2}\right]\right\} \quad (9)$$

3.1.3. Experimental Area

In a port area, there is more ship traffic and more pollutants are discharged; the harmfulness of pollutant diffusion increases with an increase in ship traffic. Therefore, a simulation experiment for an area with a large ship-traffic flow that is close to the land can effectively represent the impact of pollutant diffusion on people and the environment. The Shenzhen West Port Area, China is such an area, as shown in Figure 4.

Figure 4. The west area of Shenzhen Port.

The left image in Figure 5 shows the trajectory of the ships at that location. The rectangular area in Figure 5 has dense traffic flow and is close to the land. The area includes a guard zone, channel, and anchorage. It is the busiest water area in the western port area of Shenzhen. This area was selected for the simulation experiment.

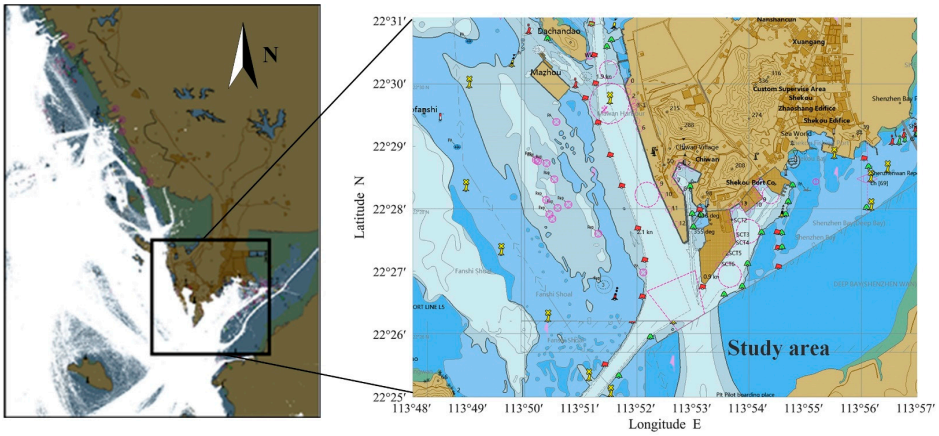

Figure 5. Study area for the diffusion simulation of exhaust gas from multiple ships.

3.1.4. Effective Source Height

In this study, the effective source height H in the Gaussian puff model is the vertical distance from the top of the ship's chimney to the sea level (referred to as the chimney height of the ship). It is difficult to obtain data about ship chimney heights, and few studies have quantified these heights. However, the height above the waterline to the highest point of the ship must exceed the ship's chimney height. Therefore, combined with above-the-waterline height data for ships in the Chinese Navigation Standard of Waterways for Seagoing Vessels (JTS 180-3-2018) and chimney height data in previous research [39], we determined the chimney heights of ships used in this study, as shown in Table 11:

Table 11. Chimney heights of different ships.

Length (m)	100<	100–200	200–300	>300
Estimated value of chimney height [1)]	12	28	43	50

Note: [1)] This value is the estimated average of the ship's chimney height in the given length interval and does not consider ship type and ship load status.

3.1.5. Meteorological Conditions

The atmospheric stability determines the diffusion coefficient, which directly affects the diffusion of ship exhaust. Furthermore, the wind speed corresponding to each level of atmospheric stability is different, which means that different wind speeds may impact exhaust gas diffusion. Using the control variable method, when the wind speed $\overline{u}$ is a variable, the variable component of Equation (9) is shown in Equation (10):

$$f(x) = \exp\left[-\frac{(x-\overline{u}(t-t_s))^2}{2\sigma_x^2}\right] \tag{10}$$

For a single puff, x is a constant value, σ_x^2 is also a constant value, and $(x-\overline{u}(t-t_s))^2 \geq 0$. For $(x-\overline{u}(t-t_s))^2 = 0$, Equation (10) has a maximum value when $x = \overline{u}t$. For the exhaust diffusion of a single puff, the historical maximum concentration value at a point downwind only relates to its downwind distance. Wind speed only affects the time when the point reaches the maximum concentration. Based on this, we analyze the impact of different atmospheric stability based on the diffusion of a single puff.

Assuming that z = 1.7 m and y = 0, we calculate the diffusion on the plane of a height of 1.7 m (close to the height of person); the effective source height H is 28 m, and Q is the discharge by a 150 m long ship within 1 s while cruising. Then we calculate the farthest distance when the NO_2 concentration decreased to 1 $\mu g/m^3$ for a single puff under the six atmospheric stabilities of A–F by the Gaussian puff model, as shown in Table 12.

Table 12. The farthest distance when the NO_2 concentration decreased to 1 $\mu g/m^3$ for a single puff.

Atmospheric Stability	A	B	C	D	E	F
Longest distance (m)	About 474	About 698	About 1052	About 1460	About 2272	About 3854

Wind speeds are respectively set at 1.9 m/s, 4.9 m/s, 5.9 m/s, 10 m/s, 4.9 m/s, 2.9 m/s for diffusion calculations A–F. At the atmospheric stability level of F, a longest distance is required for the NO_2 concentration decreased to 1 $\mu g/m^3$. As such, this paper selects the atmospheric stability of F for the simulation experiment.

3.2. Results

The concentration at any point (x, y, z) in the area is considered equivalent to the superposition of several puffs discharged by different ships at very short time intervals. Due to the continuous ship activities in the study area, there may be such situations when the puff emitted by the previous ship is not completely diffused, and/or when another ship at the position starts to emit a new puff. When there are frequent vessel activities in the port area, the concentration distributions in the study area are assumed to be relatively stable.

AIS data from 0:00 to 3:00 on 1 January 2018 are used for the calculations. The atmospheric stability is F; the wind direction is due west; and the wind speed is 2.9 m/s. The concentration distribution at 1:00, 2:00, and 3:00 is used to reflect the accumulated NO_2 concentration emitted by all ships in the study area under the action of wind within 1 h, 2 h, and 3 h. The results are shown in Figures 6–8.

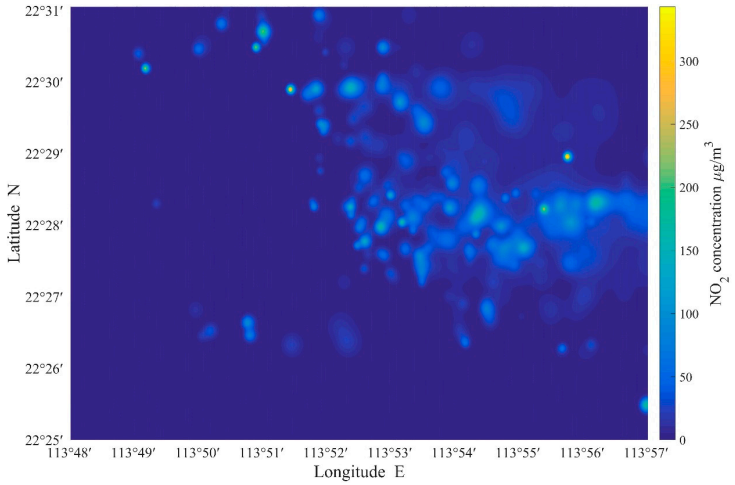

Figure 6. NO_2 concentration distribution at 1:00.

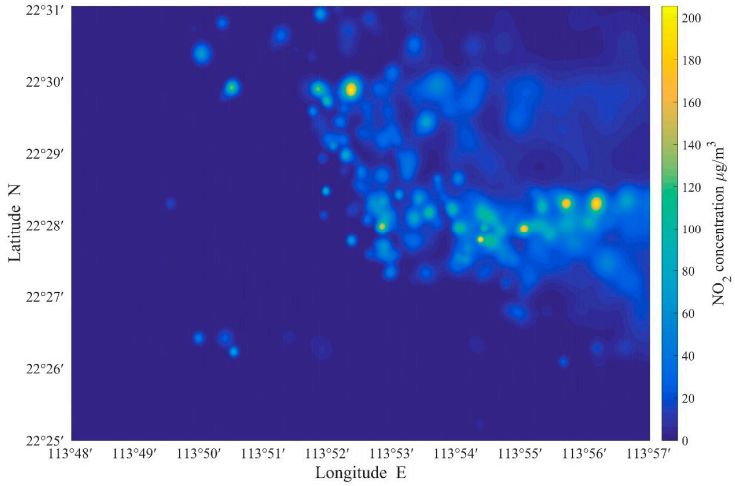

Figure 7. NO_2 concentration distribution at 2:00.

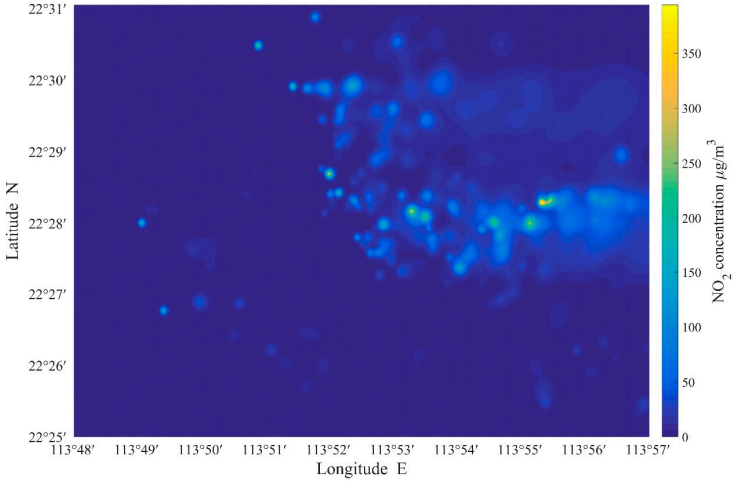

Figure 8. NO_2 concentration distribution at 3:00.

The simulated NO_2 diffusion of the exhaust from multiple ships within 1 h, 2 h, and 3 h shows that the pollutant distribution in the studied area differs at the three times. This means the distribution of the NO_2 concentration in the studied area is not stable. Since the ship exhaust concentration gradually approaches zero after a specific period of time after the exhaust is discharged, the cumulative calculation of a larger time is of little significance.

In addition, there are two explanations for the difficulty in achieving a relatively stable NO_2 concentration distribution. (1) In practice, meteorological conditions are complex and changeable, which can make the direction of exhaust gas diffusion change. (2) The carrying capacity of the western port area of Shenzhen is close to the upper limit, making it difficult to continue to increase the number of ships arriving at the port. At the same time, due to the increasing emphasis on environmental protection, ship emissions in the port area decrease.

It can be seen that the concentration distributions of Figures 6–8 are different. In other words, the concentration distribution is not stable in time. It indicates that the diffusion of exhaust from multiple ships exhaust does not have a constant impact on the port environment. However, the diffusion of exhaust from multiple ships still impacts the port area. For this, the NO_2 concentration distribution is screened at three times, at concentrations of 50 μg/m^3 and 100 μg/m^3, respectively, as shown in Figures 9–14.

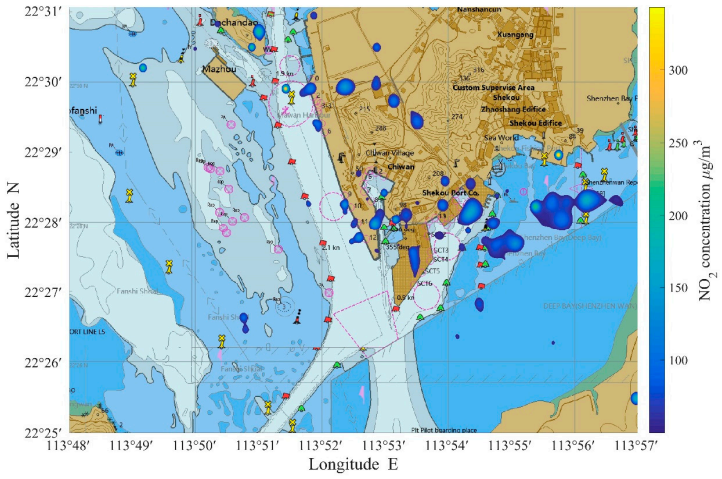

Figure 9. NO_2 concentration distribution at 1:00 (greater than 50 μg/m^3).

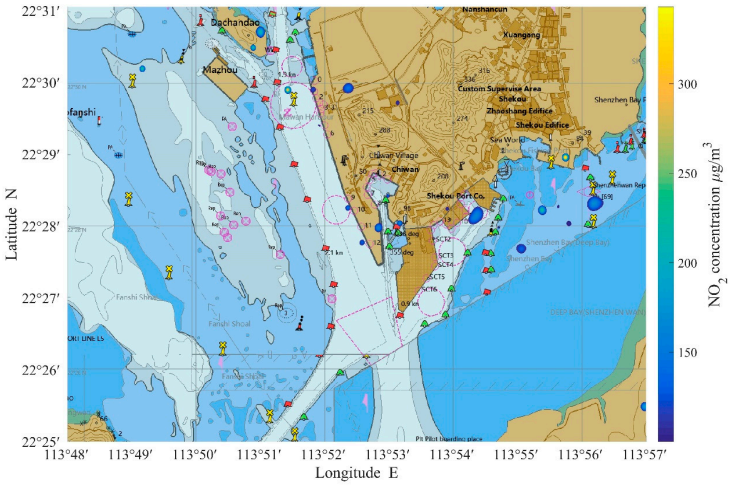

Figure 10. NO_2 concentration distribution at 1:00 (greater than 100 μg/m^3).

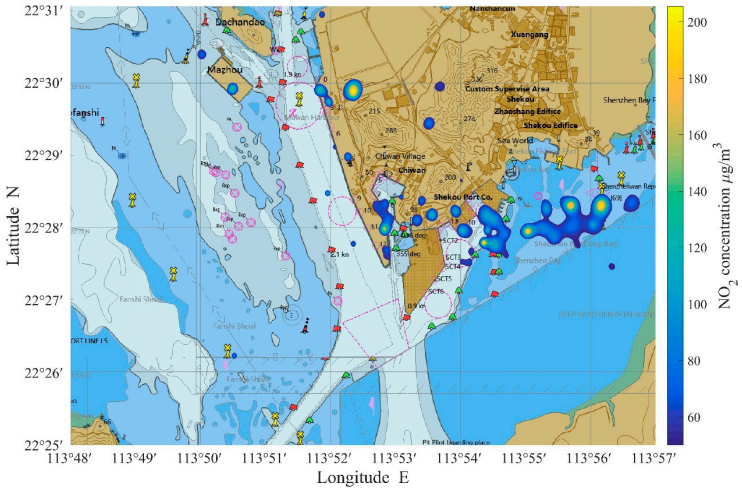

Figure 11. NO_2 concentration distribution at 2:00 (greater than 50 μg/m^3).

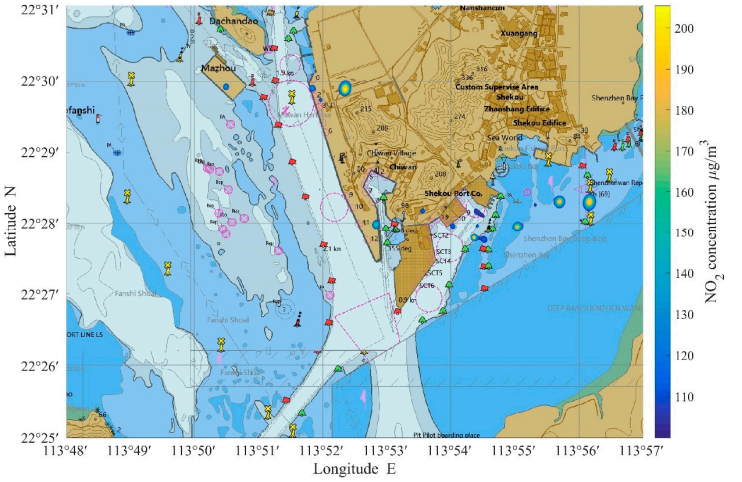

Figure 12. NO_2 concentration distribution at 2:00 (greater than 100 μg/m^3).

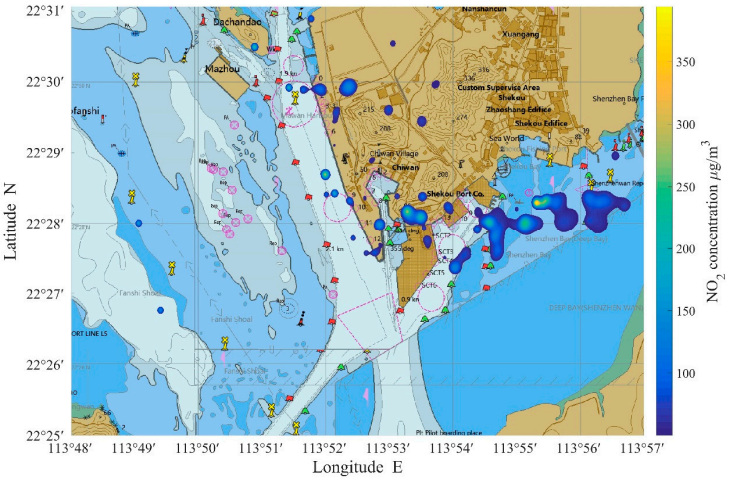

Figure 13. NO_2 concentration distribution at 3:00 (greater than 50 μg/m^3).

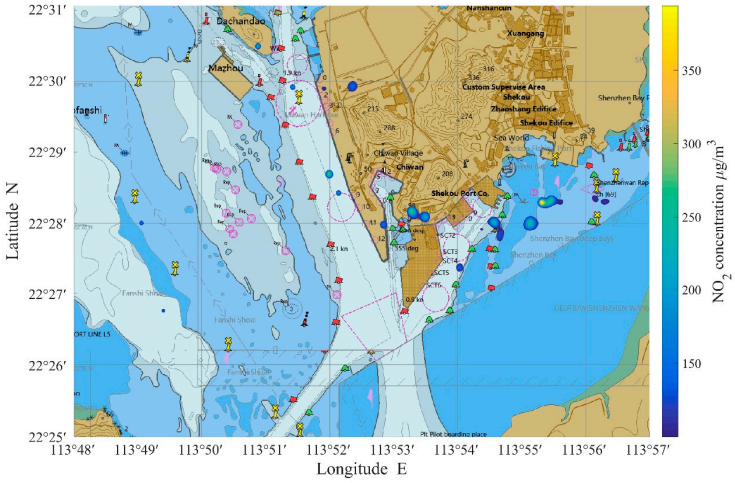

Figure 14. NO_2 concentration distribution at 3:00 (greater than 100 $\mu g/m^3$).

The figure above reflects the concentration distribution of NO_2 on a plane having a height z = 1.7 m; this height is close to human height and therefore reflects the impact of ship exhaust gas diffusion in the port area on people. This part of the study involved screening the concentration distribution of pollutant diffusion in the port area. Using a simulation with NO_2 concentrations exceeding 100 $\mu g/m^3$ (slight pollution), Figures 10, 12 and 14 show the area where the human body is significantly affected by the diffusion of the exhaust gas at this concentration from many ships in the port area. The affected area is essentially the same at the three times assessed; the affected areas are close to the sea, and they have large ship berths. Due to the large exhaust emissions of large ships, the contribution to the diffusion is also large. However, the areas with concentrations greater than 100 $\mu g/m^3$ mainly affect the environment near the port area and do not extend deep into the land area. This limits the impact on the whole study area.

When screening the concentration distribution of pollutant diffusion in the port area obtained by simulating NO_2 concentrations greater than 50 $\mu g/m^3$ (good air quality) (Figures 9, 11 and 13), the figure shows there is a smaller area where the concentration of NO_2 is greater than 50 $\mu g/m^3$. The impact of this concentration on the human body is not significant, and the impact on the study area is limited. The affected area is also caused by the diffusion of exhaust emissions from large ships in the port area.

In conclusion, the diffusion of exhaust gas from multiple ships impacts some areas near large ship berths seriously at night, and there is a small impact on the urban ecological environment and the health of residents in the western area of Shenzhen. However, it is necessary to pay attention to the daily protection of operators in the port area and residents near the port area, and reasonable air pollution control measures are needed.

4. Discussion

With the rapid development of the world shipping industry, maritime traffic brings serious problems of ship pollution [40,41]. Ship exhaust gas has become an essential source of air pollution, which impacts the ecological environment and people's health. In a port area, there is more ship traffic and more pollutants are discharged, with an increase in the harmfulness of pollutant diffusion. To assess the impact of ship exhaust emission on the atmospheric environment and human health, this paper studies the problem of ship exhaust gas diffusion in the port area, which is most effective to analyze the harm to the port area caused by the diffusion of ship exhaust gas.

The issue of ship emissions has attracted researchers for many years. Most studies have mainly focused on establishing ship emission inventories around the world. The frequent methods of establishing ship emission inventories are the top–down method and bottom–up method. The earliest ship emissions were calculated based on the top–down method [10], which involved multiplying the total fuel consumption and emission factors

to calculate ship emissions [9]. This method has been used in many studies to calculate ship emissions [11,42]. However, it is difficult to estimate the spatiotemporal characteristics of ship emissions by the top–down method. The "bottom–up" method calculates the ship emissions for each individual ship traveling between the successive AIS positions, which considers the ship engine's power, fuel consumption rate, and emissions factor. The bottom–up method is proven to be more accurate [33]. Researchers most commonly use the bottom–up method to investigate exhaust emissions in recent years [13,16–18]. This study also uses this method to calculate ship emissions and refers to parameters from the relevant research [13,32,35], but most studies have mainly focused on emissions and the emission contribution rate, and the pollution transfer effect of ship exhaust emission diffusion on land has not been explored. Some studies used the Gaussian model to analyze the atmospheric diffusion of single-ship exhaust gas [22,23,25], but these studies focused on the diffusion of single-ship exhaust with limited data, which is not enough to reflect the impact of ship exhaust gas on the environment. Therefore, research on the diffusion of multi-ship exhaust gas is needed. Based on the calculation of ship emissions, the main work of this paper is a further study on the impact of exhaust gas diffusion on port air quality; the diffusion of exhaust gas discharged by all ships is calculated based on the Gaussian puff model.

This paper studies the problem of ship exhaust gas diffusion in the port area. The results can reflect the impact of ship exhaust gas on the ecological environment and human health, lay a foundation for monitoring ship emissions, and conduce to treat the atmospheric environment of the port area in the future.

Like all studies, this one has limitations, which could be further discussed and improved in future research. First, when analyzing the diffusion of ship exhaust gas in the port area, this study does not give enough consideration to the topographic factors of the port area and the physical and chemical changes of the gas during exhaust gas diffusion. This impacts the calculation of exhaust gas diffusion. Second, ship exhaust emission is continuous, but in this study the puffs corresponding to the ship diffusion are calculated using the AIS interval, which is discretized. Finally, field experiments would be useful for verifying the simulation results in follow-up research. Despite these limitations, this study adds value to monitoring and treating the atmospheric environment by analyzing the harm to the port area caused by the diffusion of multiple ships' exhaust gas.

5. Conclusions

This paper studies the problem of ship exhaust gas diffusion in the port area. A case study is conducted to analyze the harm to the western area of Shenzhen Port caused by the diffusion of ship exhaust gas. AIS data from 0:00 to 3:00 on 1 January 2018 are used for the calculations and NO_2 is selected as the pollutant for this simulation. According to automatic identification system (AIS) data, ship exhaust gas is estimated based on the bottom-up method, and the result of emission calculation is entered into a Gaussian puff model to calculate the superposition of the diffusion of gaseous pollutants from multiple ships in the port area. The results show that the diffusion of exhaust gas from multiple ships have a bad effect on the atmospheric environment and human health under the specific conditions of this study, and the diffusion of exhaust gas mainly affects some areas near large ship berths. The simulation experiment has limitations that only three hours of a particular day were studied and a more extensive diffusion conditions were not calculated. Although it has these limitations, the conditions of this study are one of daily meteorological conditions, the results under these conditions can still reveal the impact of ship exhaust gas on human health. It is necessary to pay attention to the daily protection of operators in the port area and residents near the port area, and reasonable air control pollution measures are needed. This paper analyzes the impact on the whole western area of Shenzhen Port caused by the diffusion of ship exhaust gas, which lays a foundation for monitoring and treating the atmospheric environment in the port area.

In future research, the application of the diffusion of exhaust gas from ships in a port area will be further studied based on enriching AIS data through interpolation. Based on the constructed diffusion model of ships in the port area, there will be given more consideration to the topographic factors of the port area and the physical and chemical changes of gaseous pollutants. With these improvements, it will make rendering the diffusion simulation more accurate and improve the effect of monitoring and treating the atmospheric environment in the port area.

Author Contributions: Conceptualization, L.G.; Data curation, L.G.; Formal analysis, T.L.; Methodology, T.L. and Y.S.; Resources, L.G.; Software, T.L. and Y.S.; Supervision, L.G. and Y.S.; Validation, Y.S.; Visualization, T.L. and Y.S.; Writing—original draft, T.L. and Y.S.; Writing—review & editing, L.G. and Y.S. All authors have read and agreed to the published version of the manuscript.

Funding: This research received no external funding.

Institutional Review Board Statement: Not applicable.

Informed Consent Statement: Not applicable.

Data Availability Statement: Not applicable.

Conflicts of Interest: The authors declare no conflict of interest.

Appendix A

Table A1. Correction Multiplier of Emission Factors.

Load	SO_2	NO_x	PM	HC	CO
1.00%	1	11.47	19.17	59.28	19.32
2.00%	1	4.63	7.29	21.18	9.68
3.00%	1	2.92	4.33	11.68	6.46
4.00%	1	2.21	3.09	7.71	4.86
5.00%	1	1.83	2.44	5.61	3.89
6.00%	1	1.6	2.04	4.35	3.25
7.00%	1	1.45	1.79	3.52	2.79
8.00%	1	1.35	1.61	2.95	2.45
9.00%	1	1.27	1.48	2.52	2.18
10.00%	1	1.22	1.38	2.18	1.96
11.00%	1	1.17	1.3	1.96	1.79
12.00%	1	1.14	1.24	1.76	1.64
13.00%	1	1.11	1.19	1.6	1.52
14.00%	1	1.08	1.15	1.47	1.41
15.00%	1	1.06	1.11	1.36	1.32
16.00%	1	1.05	1.08	1.26	1.24
17.00%	1	1.03	1.06	1.18	1.17
18.00%	1	1.02	1.04	1.11	1.11
19.00%	1	1.01	1.02	1.05	1.05
20.00%	1	1	1	1	1

Table A2. Value of ship emission factor (g/kWh).

	Engine Type	Fuel Type	Sulfur Content	Pollutant					
				SO_2	NOx	PM_{10}	$PM_{2.5}$ [1)]	HC [2)]	CO
Ocean ship/Coastal ship	Medium speed (ME)	**HFO**	2.70%	10.29	18.10	1.42	1.31	0.60	1.40
		MDO	1.00%	3.62	17.00	0.45	0.42	0.60	1.40
		MGO	0.50%	1.81	17.00	0.31	0.28	0.60	1.40
	Low speed (ME)	HFO	2.70%	11.24	14.00	1.43	1.32	0.50	1.10
		MDO	1.00%	3.97	13.20	0.47	0.43	0.50	1.10
		MGO	0.50%	1.98	13.20	0.31	0.29	0.50	1.10
	AE	HFO	2.70%	11.98	14.70	1.44	1.32	0.40	1.10
		MDO	1.00%	4.24	13.90	0.49	0.45	0.40	1.10
		MGO	0.50%	2.12	13.90	0.32	0.29	0.40	1.10

Table A2. *Cont.*

	Engine Type	Fuel Type	Sulfur Content	Pollutant					
				SO_2	NOx	PM_{10}	$PM_{2.5}$ [1)]	HC [2)]	CO
Inland ship	ME [3)]	MGO	0.50%	2.08	10.00	0.30	0.29	0.27	1.50
	ME [4)]	MGO	0.50%	2.08	13.20	0.72	0.70	0.50	1.10
	ME [5)]	MGO	0.50%	2.08	13.20	0.31	0.29	0.47	1.10
	AE [6)]	MGO	0.50%	2.08	10.00	0.40	0.39	0.27	1.70
	AE [5)]	MGO	0.50%	2.12	10.00	0.31	0.29	0.26	1.50

In the table, HFO is heavy fuel oil; MDO is marine diesel oil; and MGO is marine gas oil. Note: [1)] calculate the mass ratio of $PM_{2.5}$ and PM_{10} as 0.92 to estimate the $PM_{2.5}$ emission; [2)] calculate the mass ratio of VOCs and HC as 1.053 to estimate VOC emissions; [3)] applies to other inland ships, except chemical ships, gas ships, oil tankers, and tugs; [4)] applies to chemical ships, gas ships, oil tankers, and tugs; [5)] applies to an inland passenger ferry; [6)] applies to other inland ships, except an inland passenger ferry.

Table A3. Emission factors of fishing vessels.

Type	SO_2	NO_x	CO	PM_{10} [1)]	HC [2)]
Inland ship	30.0	46.3	8.8	2.4	4.6
Coastal ship	30.0	60.1	7.0	2.4	3.2
Average	30.0	53.2	7.9	2.4	3.9

Note: [1)] calculate the mass ratio of $PM_{2.5}$ and PM_{10} as 0.92 to estimate the $PM_{2.5}$ emission; [2)] calculate the mass ratio of VOCs and HC as 1.053 to estimate VOC emissions.

References

1. UNCTAD. Review of Maritime Transport 2017. 2017. Available online: https://unctad.org/system/files/official-document/rmt2017_en.pdf (accessed on 10 December 2022).
2. Song, S. Ship emissions inventory, social cost and eco-efficiency in Shanghai Yangshan port. *Atmos. Environ.* **2014**, *82*, 288–297. [CrossRef]
3. Sampson, H.; Bloor, M.; Baker, S.; Dahlgren, K. Greener shipping? A consideration of the issues associated with the introduction of emission control areas. *Marit. Policy Manag.* **2016**, *43*, 295–308. [CrossRef]
4. Ma, W.; Lu, T.; Ma, D.; Wang, D.; Qu, F. Ship route and speed multi-objective optimization considering weather conditions and emission control area regulations. *Marit. Policy Manag.* **2021**, *48*, 1053–1068. [CrossRef]
5. Ma, W.; Hao, S.; Ma, D.; Wang, D.; Jin, S.; Qu, F. Scheduling decision model of liner shipping considering emission control areas regulations. *Appl. Ocean. Res.* **2021**, *106*, 102416. [CrossRef]
6. Ma, D.; Ma, W.; Jin, S.; Ma, X. Method for simultaneously optimizing ship route and speed with emission control areas. *Ocean. Eng.* **2020**, *202*, 107170. [CrossRef]
7. Collins, B.; Sanderson, M.G.; Johnson, C.E. Impact of increasing ship emissions on air quality and deposition over Europe by 2030. *Meteorol. Z.* **2009**, *18*, 25. [CrossRef] [PubMed]
8. Liu, H.; Fu, M.; Jin, X.; Shang, Y.; Shindell, D.; Faluvegi, G.; Shindell, K.; He, K. Health and climate impacts of ocean-going vessels in East Asia. *Nat. Clim. Change* **2016**, *6*, 1037–1041. [CrossRef]
9. Song, S.K.; Shon, Z.H. Current and future emission estimates of exhaust gases and particles from shipping at the largest port in Korea. *Environ. Sci. Pollut. Res.* **2014**, *21*, 6612–6622. [CrossRef]
10. Corbett, J.J.; Fischbeck, P.S.; Pandis, S.N. Global nitrogen and sulfur inventories for oceangoing ships. *J. Geophys. Res. Atmos.* **1999**, *104*, 3457–3470. [CrossRef]
11. Endresen, Ø.; Sørgård, E.; Behrens, H.L.; Brett, P.O.; Isaksen, I.S. A historical reconstruction of ships' fuel consumption and emissions. *J. Geophys. Res. Atmos.* **2007**, *112*. [CrossRef]
12. Jalkanen, J.P.; Johansson, L.; Kukkonen, J.; Brink, A.; Kalli, J.; Stipa, T. Extension of an assessment model of ship traffic exhaust emissions for particulate matter and carbon monoxide. *Atmos. Chem. Phys.* **2012**, *12*, 2641–2659. [CrossRef]
13. Ng, S.K.; Loh, C.; Lin, C.; Booth, V.; Chan, J.W.; Yip, A.C.; Li, Y.; Lau, A.K. Policy change driven by an AIS-assisted marine emission inventory in Hong Kong and the Pearl River Delta. *Atmos. Environ.* **2013**, *76*, 102–112. [CrossRef]
14. Jalkanen, J.P.; Johansson, L.; Kukkonen, J. A comprehensive inventory of the ship traffic exhaust emissions in the Baltic Sea from 2006 to 2009. *Ambio* **2014**, *43*, 311–324. [CrossRef] [PubMed]
15. Xing, H.; Duan, S.L.; Liang, B.N.; Liu, Q.A. Methods to estimate exhaust emissions from sea-going ships according to operational data. *Navig. China* **2016**, *39*, 93–98.
16. Jalkanen, J.P.; Brink, A.; Kalli, J.; Pettersson, H.; Kukkonen, J.; Stipa, T. A modelling system for the exhaust emissions of marine traffic and its application in the Baltic Sea area. *Atmos. Chem. Phys.* **2009**, *9*, 9209–9223. [CrossRef]
17. Fan, Q.; Zhang, Y.; Ma, W.; Ma, H.; Feng, J.; Yu, Q.; Yang, X.; Chen, L. Spatial and seasonal dynamics of ship emissions over the Yangtze River Delta and East China Sea and their potential environmental influence. *Environ. Sci. Technol.* **2016**, *50*, 1322–1329. [CrossRef]

18. Wan, Z.; Ji, S.; Liu, Y.; Zhang, Q.; Chen, J.; Wang, Q. Shipping emission inventories in China's Bohai Bay, Yangtze River Delta, and Pearl River Delta in 2018. *Mar. Pollut. Bull.* **2020**, *151*, 110882. [CrossRef]
19. He, S.; Wu, X.; Wang, J.; Guo, J. A ship emission diffusion model based on translation calculation and its application on Huangpu River in Shanghai. *Comput. Ind. Eng.* **2022**, *172*, 108569. [CrossRef]
20. Nagendra, S.; Khare, M.; Gulia, S.; Vijay, P.; Chithra, V.S.; Bell, M.; Namdeo, A. Application of ADMS and AERMOD models to study the dispersion of vehicular pollutants in urban areas of India and the United Kingdom. *WIT Trans. Ecol. Environ.* **2012**, *157*, 3–12.
21. Byun, D.; Schere, K.L. Review of the governing equations, computational algorithms, and other components of the Models-3 Community Multiscale Air Quality (CMAQ) modeling system. *Appl. Mech. Rev.* **2006**, *59*, 51–77. [CrossRef]
22. Ariana, M.; Pitana, T.; Artana, K.B.; Dinariyana, B.; Masroeri, A.A. Gaussian plume and puff model to estimate ship emission dispersion by combining automatic identification system (AIS) and geographic information system (GIS). *J. Marit. Res.* **2013**, *3*, 1–13.
23. Bai, S.; Wen, Y.; He, L.; Liu, Y.; Zhang, Y.; Yu, Q.; Ma, W. Single-vessel plume dispersion simulation: Method and a case study using CALPUFF in the Yantian port area, Shenzhen (China). *Int. J. Environ. Res. Public Health* **2020**, *17*, 7831. [CrossRef] [PubMed]
24. Murena, F.; Mocerino, L.; Quaranta, F.; Toscano, D. Impact on air quality of cruise ship emissions in Naples, Italy. *Atmos. Environ.* **2018**, *187*, 70–83. [CrossRef]
25. Peng, X.; Wen, Y.; Xiao, C.; Huang, L.; Zhou, C.; Zhang, F.; Zhang, Y. Improved calculation model for ship exhaust emission dispersion. *J. Saf. Environ.* **2020**, *20*, 255–264. Available online: https://zhikuyun.xinhua.org/Liems/web/result/detail.htm?index=cgk_journal&type=achievement&id=CJFDAUTO_AQHJ202001034 (accessed on 10 December 2022).
26. Sausen, R. Transport impacts on atmosphere and climate: The ATTICA assessment report. *Atmos. Environ.* **2010**, *44*, 4645–4816. [CrossRef]
27. Matthias, V.; Bewersdorff, I.; Aulinger, A.; Quante, M. The contribution of ship emissions to air pollution in the North Sea regions. *Environ. Pollut.* **2010**, *158*, 2241–2250. [CrossRef]
28. Sharan, M.; Yadav, A.K.; Singh, M.P. Plume dispersion simulation in low-wind conditions using coupled plume segment and Gaussian puff approaches. *J. Appl. Meteorol. Climatol.* **1996**, *35*, 1625–1631. [CrossRef]
29. Li, K.; Liang, M.; Su, G. Data assimilation method for atmospheric dispersion based on a Gaussian puff model. *J. Tsinghua Univ. (Sci. Technol.)* **2018**, *58*, 992–999.
30. Liu, Y.; Lu, W.; Wang, H.; Huang, Q.; Gao, X. Odor impact assessment of trace sulfur compounds from working faces of landfills in Beijing, China. *J. Environ. Manag.* **2018**, *220*, 136–141. [CrossRef]
31. Herrería-Alonso, S.; Suárez-González, A.; Rodríguez-Pérez, M.; Rodríguez-Rubio, R.F.; López-García, C. A solar altitude angle model for efficient solar energy predictions. *Sensors* **2020**, *20*, 1391. [CrossRef]
32. Zhu, Q.; Liao, C.; Wang, L.; Han, H.; Liu, J.; Zhang, Y.; Zeng, W. Application of fine vessel emission inventory compilation method based on AIS data. *China Environ. Sci.* **2017**, *37*, 4493–4500.
33. Chen, D.; Wang, X.; Li, Y.; Lang, J.; Zhou, Y.; Guo, X.; Zhao, Y. High-spatiotemporal-resolution ship emission inventory of China based on AIS data in 2014. *Sci. Total Environ.* **2017**, *609*, 776–787. [CrossRef] [PubMed]
34. Ng SK, W.; Lin, C.; Chan, J.W.M. Study on marine vessels emission inventory, final report. *Hong Kong China Hong Kong Environ. Prot. Dep.* **2012**, *2012*, 9–103.
35. Yang, J.; Yin, P.L.; Si-Qi, Y.; Wang, S.S.; Zheng, J.Y.; Ou, J.M. Marine emission inventory and its temporal and spatial characteristics in the city of Shenzhen. *Environ. Sci.* **2015**, *36*, 1217–1226.
36. Guo, H.; Gu, X.; Ma, G.; Shi, S.; Wang, W.; Zuo, X.; Zhang, X. Spatial and temporal variations of air quality and six air pollutants in China during 2015–2017. *Sci. Rep.* **2019**, *9*, 15201. [CrossRef]
37. Gan, L.; Che, W.; Zhou, M.; Zhou, C.; Zheng, Y.; Zhang, L.; Rangel-Buitrago, N.; Song, L. Ship exhaust emission estimation and analysis using Automatic Identification System data: The west area of Shenzhen port, China, as a case study. *Ocean. Coast. Manag.* **2022**, *226*, 106245. [CrossRef]
38. Sun, W.Y.; Ding, S.L.; Zeng, S.S.; Su, S.J.; Jiang, W.J. Simultaneous absorption of NOx and SO2 from flue gas with pyrolusite slurry combined with gas-phase oxidation of NO using ozone. *J. Hazard. Mater.* **2011**, *192*, 124–130. [CrossRef]
39. Mocerino, L.; Murena, F.; Quaranta, F.; Toscano, D. A methodology for the design of an effective air quality monitoring network in port areas. *Sci. Rep.* **2020**, *10*, 1–10. [CrossRef] [PubMed]
40. Chen, Q.; Lau, Y.Y.; Ge, Y.E.; Dulebenets, M.A.; Kawasaki, T.; Ng, A.K. Interactions between Arctic passenger ship activities and emissions. *Transp. Res. Part D Transp. Environ.* **2021**, *97*, 102925. [CrossRef]
41. Shu, Y.; Wang, X.; Huang, Z.; Song, L.; Fei, Z.; Gan, L.; Xu, Y.; Yin, J. Estimating spatiotemporal distribution of wastewater generated by ships in coastal areas. *Ocean. Coast. Manag.* **2022**, *222*, 106133. [CrossRef]
42. Kesgin, U.; Vardar, N. A study on exhaust gas emissions from ships in Turkish Straits. *Atmos. Environ.* **2001**, *35*, 1863–1870. [CrossRef]